Journal of Zhejiang University-SCIENCE A (Applied Physics & Engineering)
ISSN 1673-565X (Print); ISSN 1862-1775 (Online)
www.zju.edu.cn/jzus; www.springerlink.com
E-mail: jzus@zju.edu.cn

Numerical analysis of pipeline in J-lay problem*

Li-zhong WANG, Feng YUAN†‡, Zhen GUO, Ling-ling LI

(*College of Civil Engineering and Architecture, Zhejiang University, Hangzhou 310058, China*)

†E-mail: yuanfen5742@163.com

Received Dec. 19, 2009; Revision accepted May 14, 2010; Crosschecked Oct. 12, 2010

Abstract: The pipe configuration and internal loads along the pipeline during the pipeline laying process have long been the focus of engineers. Most researchers simplify the seabed to be rigid and the water to be calm, ignoring the pipe embedment into the seabed and the influence of ocean currents. In this paper, a novel numerical approach is proposed for the laying of pipelines in the so-called J-lay method, taking into account the importance of both pipe embedment and ocean currents. The pipeline is divided into two parts, one part suspended in water, and the other laid on the seabed. The continuity of the two parts at the touch down point (TDP) is guaranteed to make a whole. The feasibility of the model is proved by the comparison between the present model and an analytical model, which shows good agreement in both pipeline configuration and bending moment distribution. Finally, parametric study was performed to consider the influence of current velocity, water depth, top inclination angle, and seabed stiffness, and conclusions are drawn.

Key words: Pipeline, J-lay method, Numerical model, Seabed stiffness, Current velocity
doi:10.1631/jzus.A0900773 **Document code:** A **CLC number:** TE3

1 Introduction

In recent decades, the increased demand for natural resources has driven the exploration of oil and gas fields to deepwater or even ultra-deepwater. In deepwater, pipelines have been by far the most efficient and economical means of large scale transportation for crude oil and natural gas. Within deepwater, the environment is more complicated and more hazards arise, making the laying of pipelines challenging. Most pipelines encounter their highest stresses during the laying process (Powers and Finn, 1969; Brando and Sebastiani, 1971). To keep up with the development of explorations in deepwater, a new installation method has become available: the J-lay method. As shown in Fig. 1, compared with the conventional S-lay method, the J-lay method is more suitable for deepwater and ultra-deepwater because of its particular advantages. First, less horizontal force is needed for maintaining station. Moreover, no stinger is required to provide the initial bending moment at the top, and the touch down point (TDP) is closer to the laying barge, which makes positioning and monitoring easier (Li *et al*., 2008). At present, considerable laying of steel catenary riser in deepwater is being accomplished by the J-lay method. Lenci and Callegari (2005) considered the J-lay method to be the most appropriate technique for installations in deepwater. Liang (2008) pointed out that the J-lay method is the only feasible way to lay pipelines in some cases. As new oilfields are explored and developed in deeper and deeper water, the J-lay method has thus attracted more and more attention.

The configuration and internal loads along the pipe have been focus of researchers because they are closely related with the layability of pipelines. Following the seminal work of Wasow (1956), Plunkett (1967) used the singular perturbation method to derive asymptotic expansion, and thereby deal with the behavior of stiffened catenary, considering the boundary layers. Dixon and Rutledge (1968) applied

‡ Correspongding auther
* Project (No. 50779061) supported by the National Natural Science Foundation of China

Plunkett's expansions to the analysis of the J-lay method. Palmer *et al*. (1974), Guarracino and Mallardo (1999), and Zhou (2008) developed the expansions to analyze the S-lay method. The method of asymptotic expansion has proved an important approach, but it is not able to consider the effect of ocean currents and pipe embedment. Pipe embedment is important because it not only influences the load distribution but also determines the initial condition of further movement of pipelines in service, such as buckling and walking. Thus, much work has been done on this subject (Murff *et al*., 1989; Aubeny *et al*., 2006; Cheuk *et al*., 2008; Merifield *et al*., 2008; 2009). Considering the importance of seafloor interaction, Pulici *et al*. (2003) presented a finite element modeling of the J-lay method which considered the pipeline embedment based on the experience accumulated in the Blue Stream Project, which tends to transport gas from Russia to Turkey. Lenci and Callegari (2005) investigated some analytical models to reveal the theoretical basis of the J-lay problem. However, the solution is not easy to obtain because the equations in their models are highly nonlinear. Moreover, the influence of ocean currents cannot be considered. The importance of ocean currents has been demonstrated by many investigations into the cable installation problem (Casarella and Parsons, 1970; Burgess, 1994; Vaz and Paten, 2000), but it is seldom considered in the pipeline laying process. Some available numerical tools take into account the influence of current and seabed embedment, and most of the tools are developed on the basis of finite element analysis. Of the available numerical tools, OFFPIPE is most frequently used. In OFFPIPE, the top tension should be assumed before calculation, which makes it less convenient for deepwater pipeline laying because the monitoring parameter in deepwater is the geometry and in particular the liftoff angle (Perinet and Frazer, 2007). In addition, commercial numerical tools are often uneconomical. The model presented in this work is based on the monitored liftoff angle, which makes it more advantageous for pipeline laying in deepwater. And the calculation of the present model requires merely several seconds on a common personal computer, but still provides reliable results. The theory of the present model can help engineers to understand the nature of the complex phenomena which characterize pipeline laying.

The aim of this paper is to present a simple numerical model for the analysis of J-lay problem. In this model, the pipeline is divided into two parts: one part suspended in water and the other laid on the seabed. To focus on the main points without redundancies, the following assumptions are made:

1. For the portion in water, the pipeline is so long that it becomes flexible. The bending moment is negligible compared with axial tension, and thus the bending stiffness can be neglected in this work. This assumption has been used in some previous work (Dixon and Rultledge, 1968; Langner, 1984).

2. Axial tension of the pipe laid on the seabed is considered constant.

3. Axial deformation of the pipe is neglected because it has little influence in practical application (Lenci and Callegari, 2005).

4. The model is restricted to the static case.

5. The laying process is considered as a planar problem only.

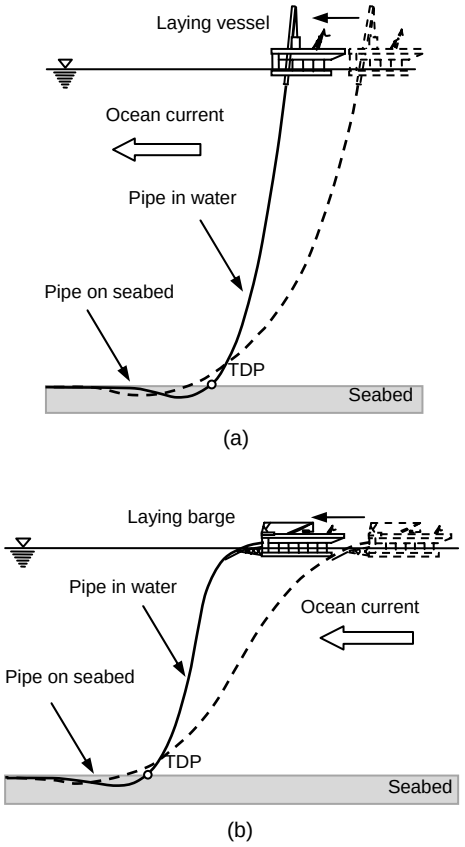

Fig. 1 Configuration of pipelines in the laying process by the J-lay method (a) and S-lay method (b)

At present, little work has been done to calculate the overall configuration for the J-lay problem, taking the pipe embedment into consideration. Furthermore, no published method takes into account the influence of ocean currents. One of the main achievements of this paper is proposing a simple numerical model taking into account the influence of ocean currents and seabed stiffness, and the importance of their influence is demonstrated.

2 Formulation of governing equations

Various mechanical features play a key role in a successful laying, such as top angle, water depth, ocean currents, seabed stiffness, etc. All these issues require appropriate modeling and must be accurately investigated.

1. Portion of pipe suspended in water

Due to the passing current and waves, the flow field around the pipe is highly complicated and hard to predict. At present, although some available numerical tools could be applied to determine the hydrodynamic loading, they are not yet economical for this application. Thus, the commonly used semi-empirical Morison's equation is adopted (Morison *et al*., 1950).

Consider a differential pipe segment of stretched length dl subjected to gravity, external hydrodynamic loading as well as its internal structural response loading (Fig. 2a).

Taking the equilibrium of the vertical force H, horizontal force V and bending moment M of this differential element and neglecting the high-order terms, the governing equations for the pipe are derived as

$$\mathrm{d}V = F_\mathrm{t}\mathrm{d}l\sin\theta - F_\mathrm{n}\mathrm{d}l\cos\theta - w\mathrm{d}l, \quad (1)$$

$$\mathrm{d}H = F_\mathrm{n}\mathrm{d}l\sin\theta + F_\mathrm{t}\mathrm{d}l\cos\theta, \quad (2)$$

$$\mathrm{d}M = V\mathrm{d}l\cos\theta - H\mathrm{d}l\sin\theta, \quad (3)$$

where θ is the inclination slope, dl is the length of a pipe segment, and w is the submerged weight of the pipe per unit length. The steady hydrodynamic forces in the normal and tangential directions F_n and F_t can be obtained by Morison's equation:

$$F_\mathrm{n} = 0.5\rho_\mathrm{w}C_\mathrm{n}D(v\sin\theta)^2, \quad (4)$$

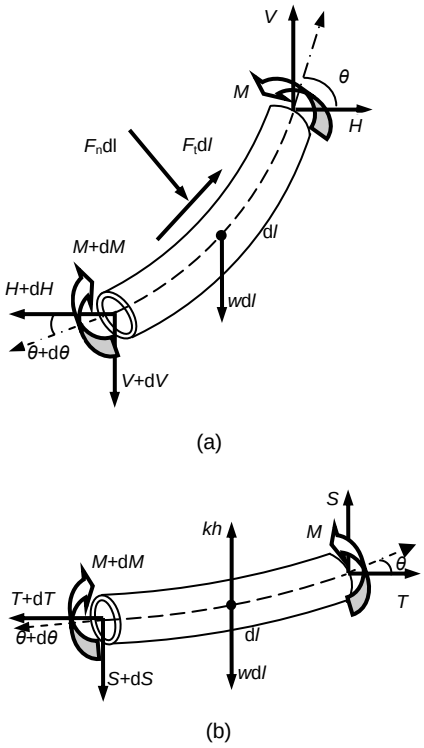

Fig. 2 Force sketch of segments of pipe in water (a) and on the seabed (b)

$$F_\mathrm{t} = 0.5\rho_\mathrm{w}C_\mathrm{t}D(v\cos\theta)^2, \quad (5)$$

where ρ_w is the density of ocean water, v is the current velocity, C_n and C_t are the drag coefficients in the normal and tangential directions, respectively.

The directions of hydrodynamic forces are closely related with the current direction. The current in Fig. 2a is in the negative x direction. If the direction changes to the positive x direction, the corresponding hydrodynamic forces in the governing equations should be replaced by $-F_\mathrm{n}$ and $-F_\mathrm{t}$, respectively.

By virtue of assumption 1, the portion in water is unable to resist the bending moment. Therefore, the direct relationship between forces and the angle θ can be extracted from Eq. (3):

$$\frac{V}{H} = \tan\theta, \quad (6)$$

where V and H are components of axial tension in vertical and horizontal directions, respectively. So the inclination angle θ is only controlled by axial tension.

Neglecting axial strain and shear strain of the pipe, the following geometric relations can be

obtained:

$$\mathrm{d}x = \mathrm{d}l\cos\theta, \tag{7}$$

$$\mathrm{d}y = \mathrm{d}l\sin\theta. \tag{8}$$

Note that although the pipe in water does not support flexure according to the assumptions of this work, the real bending moment can be approximately obtained by multiplying the bending stiffness EI and the curvature κ:

$$M = EI\kappa. \tag{9}$$

2. Portion of pipe laid on the seabed

Generally, the current velocity at the seabed is small, so the influence of ocean current could be ignored for the pipe on the seabed. But the bending moment of this portion plays an important role on the neighborhood of TDP, so it should be taken into consideration.

To guarantee the continuity of bending moment at TDP, the seabed is not considered rigid, but behaves like a Winkler foundation. The elementary beam theory is used as the basis for developing formulations for a differential segment as shown in Fig. 2b:

$$EI\frac{\mathrm{d}^4y}{\mathrm{d}x^4} - T\frac{\mathrm{d}^2y}{\mathrm{d}x^2} + k(y-h) = w, \tag{10}$$

where T is a constant tension, k is the seabed stiffness, and h is the depth from the sea level. For $T > 2\sqrt{EIk}$, no real solution can be obtained; but for $T \le 2\sqrt{EIk}$, the general solution can be obtained by

$$\begin{aligned} y = h + \frac{w}{k} + c_1\mathrm{e}^{-\alpha x}\cos(\beta x) + c_2\mathrm{e}^{-\alpha x}\sin(\beta x) \\ + c_3\mathrm{e}^{\alpha x}\cos(\beta x) + c_4\mathrm{e}^{\alpha x}\sin(\beta x), \end{aligned} \tag{11}$$

where c_1, c_2, c_3, and c_4 are unknown coefficients, and

$$\alpha = \frac{1}{2}\sqrt{2\sqrt{\frac{k}{EI}} + \frac{T}{EI}}, \tag{12}$$

$$\beta = \frac{1}{2}\sqrt{2\sqrt{\frac{k}{EI}} - \frac{T}{EI}}. \tag{13}$$

It must be noted that the inequality $T \le 2\sqrt{EIk}$ needs to be checked at the end of calculation, and it can always be satisfied by the solutions presented in the following work.

The pipe laid on the seabed is modeled as a beam on the Winkler foundation. Since it is a long distance from TDP to the anchor pile, the pipe on the seabed can be treated as a beam of infinite length. Considering the boundary condition at $x\to\infty$, where the embedment of pipe is only influenced by its self-weight and the value of y approximates $h + \frac{w}{k}$, c_3 and c_4 must be zero. Therefore, Eq. (12) can be simplified as

$$y = h + \frac{w}{k} + c_1\mathrm{e}^{-\alpha x}\cos(\beta x) + c_2\mathrm{e}^{-\alpha x}\sin(\beta x). \tag{14}$$

The associated bending moment and shear are

$$M = -EI\frac{\mathrm{d}^2y}{\mathrm{d}x^2}, \tag{15}$$

$$S = -EI\frac{\mathrm{d}^3y}{\mathrm{d}x^3}. \tag{16}$$

The geometric relations here are the same as those of pipe in water, namely Eq. (7) and Eq. (8).

3 Numerical solution

The key for numerical calculation is to obtain a reasonable top tension by continuous iteration. If the top tension is determined, the configuration and internal loads of the whole pipe can be easily determined.

3.1 Iteration process

The pipe in water is divided into n elements with the same dy along the vertical direction in the global coordinate system, and all segments are considered to be small elements without curvature, for simplicity, as shown in Fig. 3. The pipe segments are numbered by index i which ranges from 1 at the top to n at the seabed, and the corresponding ending points (EPs) of segments range from 1 to n+1.

Consider an arbitrary element i in water in Fig. 4a, the formulations of geometric and equilibrium relations can be derived:

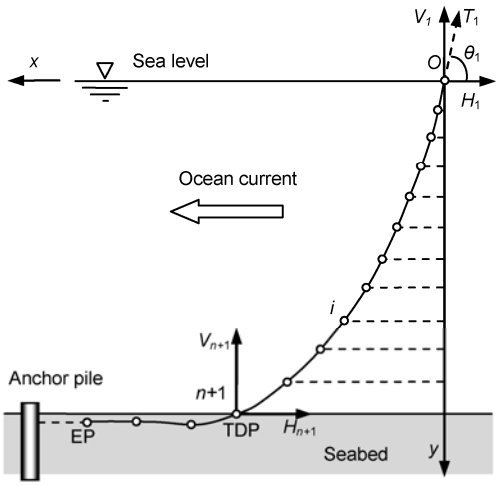

Fig. 3 Element division of the model

$$x_{i+1} = x_i + \frac{\mathrm{d}y}{\tan\theta_i}, \tag{17}$$

$$y_{i+1} = y_i + \mathrm{d}y, \tag{18}$$

$$\mathrm{d}l_i = \frac{\mathrm{d}y}{\sin\theta_i}, \tag{19}$$

$$V_{i+1} = V_i + F_{ti}\mathrm{d}l_i\sin\theta_i - F_{ni}\mathrm{d}l_i\cos\theta_i - w\mathrm{d}l_i, \tag{20}$$

$$H_{i+1} = H_i + F_{ti}\mathrm{d}l_i\cos\theta_i + F_{ni}\mathrm{d}l_i\sin\theta_i. \tag{21}$$

For pipe on the seabed, Eq. (14) should be solved to determine the two variables c_1 and c_2, which needs two boundary conditions. After that, the pipe should be divided into small segments with the same dl along its axis, as shown in Fig. 4b, to obtain the final results. Considering the boundary conditions at $x\to\infty$ have already been satisfied in Eq. (14), to guarantee the continuity at TDP, two boundary conditions, namely the continuity of coordinates and the slope at TDP, are adopted:

$$y_{\mathrm{TDP}} = h, \tag{22}$$

$$y'_{\mathrm{TDP}} = \tan\theta_{n+1}. \tag{23}$$

On the basis of Eqs. (22), (23), and (14), c_1 and c_2 can be uniquely determined for a given T_1, and then the corresponding pipe configuration and internal loads along the pipe can be obtained. For a different T_1, the results are different. However, only one group of results can guarantee the continuity of bending moment at TDP, which needs to be checked at the end of each calculation. Thus, iteration is needed to obtain

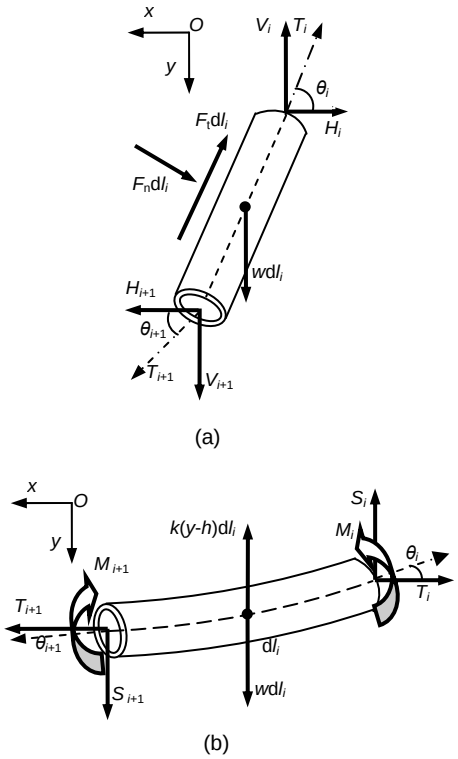

Fig. 4 Force sketch of calculation elements of pipe in water (a) and on the seabed (b)

the reasonable T_1, and when T_1 is determined, the configuration and internal loads of pipe laid on the seabed could be obtained on the basis of Eqs. (14)–(16):

$$x_{i+1} = x_i + \mathrm{d}x, \tag{24}$$

$$y_{i+1} = y|_{x=x_{i+1}}, \tag{25}$$

$$T_i = T_{n+1}, \tag{26}$$

$$M_i = -EI \times \left.\frac{\mathrm{d}^2 y}{\mathrm{d}x^2}\right|_{x=x_i}, \tag{27}$$

$$S_i = -EI \times \left.\frac{\mathrm{d}^3 y}{\mathrm{d}x^3}\right|_{x=x_i}, \tag{28}$$

where the index i begins with n+1 at the TDP, and ends at the EP, for pipe laid on the seabed.

3.2 Calculation procedure

At the beginning, basic parameters are inputs for both parts of pipe in water and on the seabed. To start the calculation of pipe in water, it is necessary to assume an initial T_1, and T_1=1.1wh is recommended

for the first step of iteration according to the following calculations. When the calculation of pipe in water is complete, verification is needed to see if the axial tension is large enough to support the self-weight of the pipe. If V_i<0 appears, T_1 must be too small and should be increased. After V_i>0 is satisfied, T_{n+1} and θ_{n+1} can then be input into Eq. (22) and Eq. (23) to determine the two unknown parameters c_1 and c_2, respectively.

Next, the bending moment along the pipe laid on the seabed can be obtained by Eq. (15). To guarantee the continuity of bending moment at TDP, $|M^+_{\mathrm{TDP}} - M^-_{\mathrm{TDP}}| < \varepsilon$ must be satisfied, where ε is a small specified quantity, M^+_{TDP} and M^-_{TDP} are both bending moments at TDP which obtained from equations of pipeline in water and on the seabed, respectively. If the bending moment is continuous, the calculation can proceed to EP which is set previously by pipe length from water level l_{EP} or the distance from the vessel in the x direction x_{EP}. The detailed process is shown in Fig. 5.

3.3 Example and comparison

1. Parameter selection

Parameters are critical for the calculation and they should be selected rationally. Table 1 shows basic parameters including the elastic modulus E, density of the sea water ρ_{w}, density of the steel pipe ρ_{p}, outer and inner diameters D and d, depth from the sea level h, inclination slope at the top θ_1, and current velocity v. The hydrodynamic parameters and the seabed stiffness are discussed in detail as follows. In addition, the water is assumed to be calm in order to make it possible to compare the results with those of Lenci and Callegari (2005).

The relationship between soil resistance R and the embedment e is nonlinear, and much work has been done to reveal the interaction mechanism between pipe and the seabed (Murff *et al*., 1989; Aubeny and Dunlap, 2003; Bridge *et al*., 2004; Aubeny *et al*., 2005; Merifield *et al*., 2008). In this work, the interaction relationship between pipe and seabed is obtained based on Aubeny *et al*. (2005) which concluded an empirical power expression:

$$\frac{R}{S_{\mathrm{u}}D} = a\left(\frac{e}{D}\right)^b, \tag{29}$$

where S_{u} is the undrained shear strength of the seabed, kPa. Coefficients a and b are related with pipe roughness and the variation of shear strength of soil.

The pipe is assumed to be rough, and the shear strength of soil varies linearly with the depth from 0 at the mudline by an increase rate η=1.5 kPa/m (Fig. 6).

The values of a and b for different cases can be determined according to (Aubeny *et al*., 2005): for e/D<0.5, the recommended values of coefficients are a=5.95 and b=0.15, so R=6.8425$D^{0.85}e^{1.15}$; for e/D

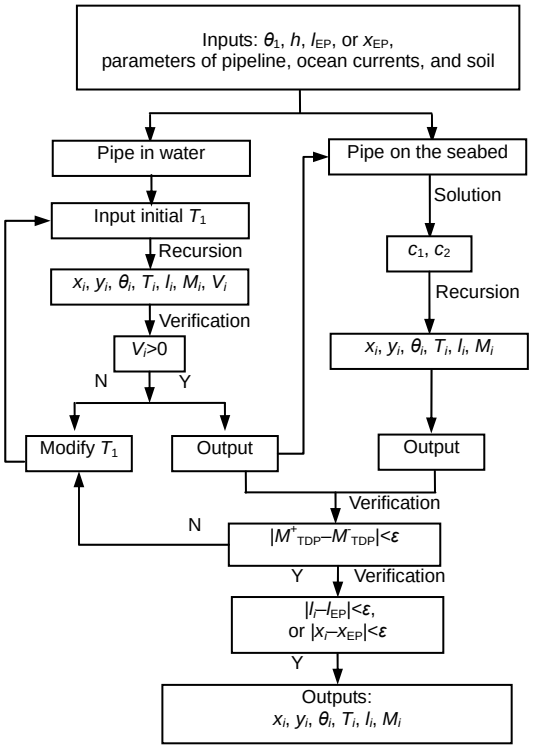

Fig. 5 Flow scheme for J-lay method calculation

Table 1 Basic parameters

E (Pa)	ρ_{w} (kg/m^3)	ρ_{p} (kg/m^3)	D (m)	d (m)	h (m)	θ_1 (°)	v (m/s)
2.1×10^{11}	1030	7850	0.60	0.55	2000	80	0

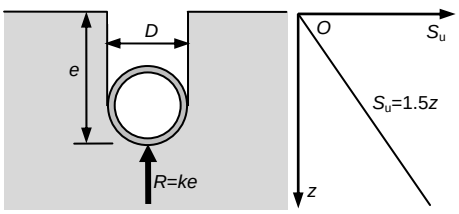

Fig. 6 Sketch of a penetrating pipe segment

>0.5, a=6.02 and b=0.20, so R=9.03$D^{0.8}e^{1.2}$, where the indexes of e, namely 1.15 and 1.2, are very close to 1, so the results can be fitted linearly with the fitting correlation coefficient up to 0.9888, as shown in Fig. 7. The fitted soil stiffness k=5.91 kN/m^2 is adopted for the following calculations, thus the soil resistance R=5.91e kN/m.

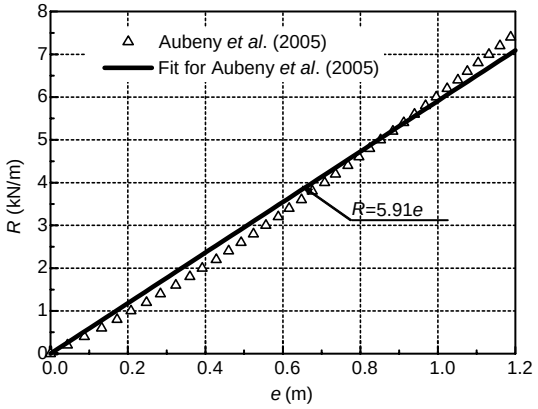

Fig. 7 Relationship between resistance and embedment for depth up to two diameters

As for the hydrodynamic parameters, the normal drag coefficient C_n depends on many factors such as Reynolds number, roughness of the pipe, and vortex induced vibration (Berteaux, 1976). C_n=1.2 is chosen in the following calculations. Wilson (1960) recommended that the ratio of C_t/C_n ranges from 0.01 to 0.03 for different cylinders and cables. In this work, C_t/C_n=0.02 is selected, so C_t=0.024.

2. Result analysis

The results of the numerical example are compared with the analytical model of Lenci and Callegari (2005). As shown in Fig. 8a, the overall configurations of pipeline calculated by the analytical model and the presented numerical model almost coincide. The configurations of the two models at the neighborhood of TDP are illustrated in Fig. 8b. The difference between the configurations may be ascribed as the influence of the boundary layer which also causes some difference in bending moments as shown in Fig. 9a. The axial tensions are almost the same, as shown in Fig. 9b. The differences between the results of the two models are shown quantatively in Table 2, where the difference percentages for M_{max}, T_{max}, T_{TDP}, and x_{TDP} are very small. Note that in the distribution curve of bending moment calculated from the presented numerical model, there is an inflection point at TDP, as shown in Fig. 9a. The inflection point is caused by a sudden change of shear force when the pipe first touches the seabed at TDP.

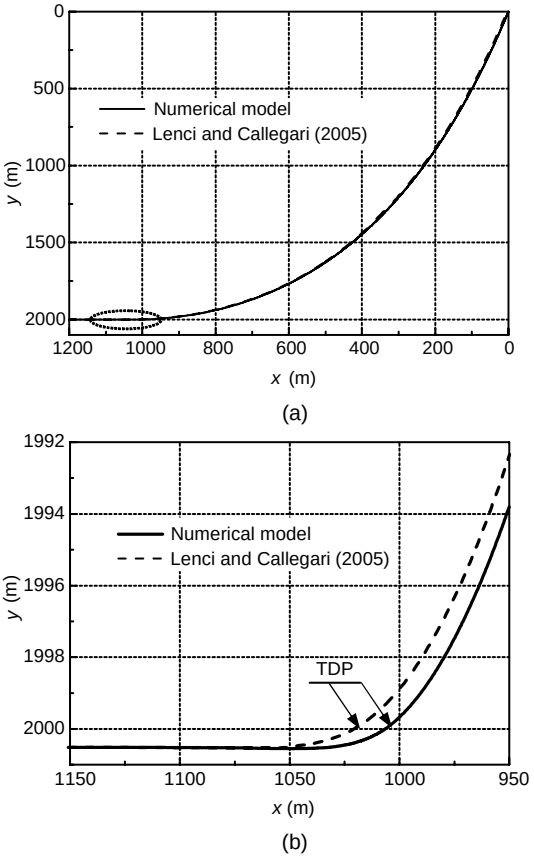

Fig. 8 Configuration comparison of overall pipeline (a) and neighborhood of TDP (b)

4 Parametric study

In this part, the effects of water depth, ocean currents, top angle, and seabed stiffness are investigated in detail to predict their influence on the internal load distribution and pipe configuration. Prediction of load distribution, especially the maximum tension and maximum bending moment, is vital for the safety of pipelines. The loads at TDP are also important because fatigue failure always occur at the neighborhood of TDP. Prediction of pipe configuration, including the distance from TDP to the laying vessel, helps the positioning of the pipeline. Moreover, the embedment of pipe is important because it determines the initial condition of further movement of pipe at work, and it is also predictable in this study.

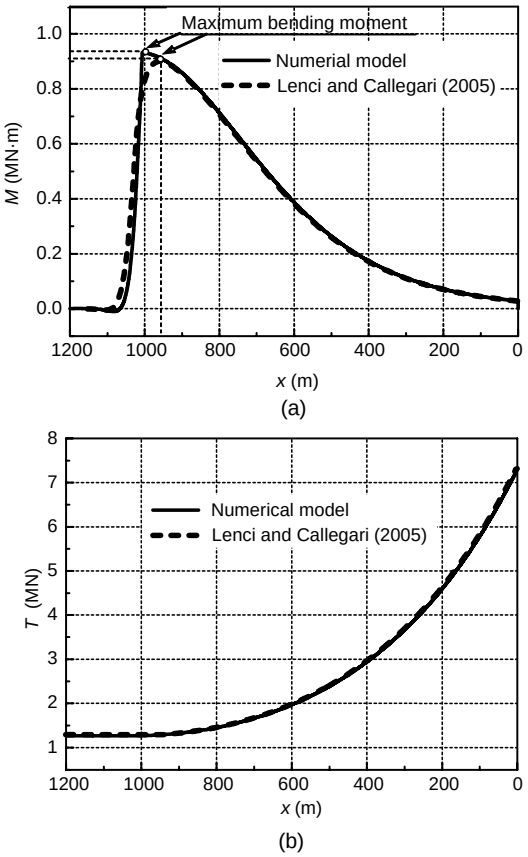

Fig. 9 Distribution of bending moment (a) and axial tension (b)

Table 2 Difference between the numerical and analytical models

Item	M_{max} (MN·m)	T_{max} (MN)	T_{TDP} (MN)	x_{TDP} (m)
Numerical model	0.93	7.31	1.27	1006.55
Analytical model	0.90	7.31	1.29	1020.80
Difference	3.33%	0%	1.57%	1.42%

4.1 Influence of water depth

One of the most attractive features of the J-lay method is its favorable applicability in deepwater and ultra-deepwater. As the water becomes deeper, the configuration and stress state of the pipeline change greatly. Four different depths are chosen for the analysis: 1000, 1500, 2000, and 2500 m. Other parameters are the same as shown in Table 1.

Fig. 10 shows the changes of the pipe profile for different depths, where the maximum pipe embedment (e_{max}) locates near TDP. The changes of forces along the pipe are shown in Fig. 11. As shown in Table 3, the distance from TDP to the laying vessel is always about half the water depth for each case, and the pipe embeds less into the soil near TDP with the increasing water depth, and the maximum embedment becomes closer to embedment at $x\to\infty$ ($e_{x\to\infty}$). Critical loads for different water depths are shown in Table 4.

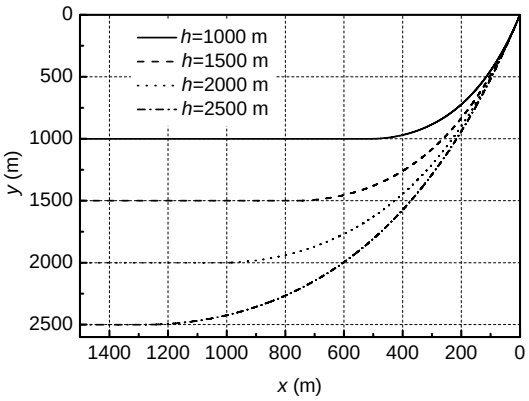

Fig. 10 Configuration of pipeline for different ocean depths

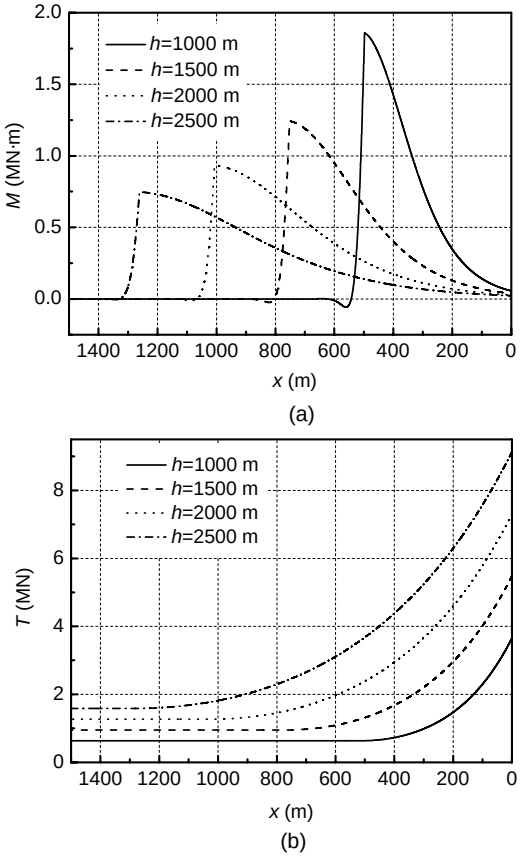

Fig. 11 Distribution of bending moment (a) and axial tension (b) for different water depths

Table 3 Distances from TDP to the vessel and pipe embedment for different water depths

Depth (m)	Distance (m)	e_{max} (m)	$e_{x\to\infty}$ (m)
1000	497.58	0.71	0.51
1500	752.00	0.60	0.51
2000	1006.55	0.55	0.51
2500	1261.19	0.53	0.51

Table 4 Critical loads for different depths

Depth (m)	M_{max} (MN·m)	T_{max} (MN)	T_{TDP} (MN)
1000	1.86	3.65	0.64
1500	1.24	5.48	0.95
2000	0.93	7.31	1.27
2500	0.75	9.13	1.59

4.2 Influence of ocean current velocity

The distribution of current velocity depends on many issues such as water depth, topography, wind, and temperature. For example, the maximum current velocity in South China Sea is generally less than 1 m/s and sometimes reaches 2 m/s. For simplicity, the distribution of current velocity is considered to vary linearly with the maximum velocity at the surface and zero at the bottom. And seven different maximum surface velocities are selected with their positive directions the same as the positive x direction: −2, −1, −0.5, 0, 0.5, 1, 2 m/s. For other parameters, please refer to Table 1.

For convenience in calculation, the EP is set by l_{EP}=1.5h. And 1.5h is enough to guarantee that the position of EP does not change with currents. Thus, the pipes in different current velocities have the same EP (Fig. 12).

Fig. 12 and Fig. 13 show the configuration and internal loads along the pipeline in different velocity distributions, respectively. Note that the bending moment for a top velocity of 2 m/s is not plotted in Fig. 13a, because its maximum bending moment M_{max} is far larger than other cases, as shown in Table 5.

Table 6 demonstrates that with increasing current velocity, TDP becomes closer to the laying vessel and the pipe embeds deeper into the soil near TDP. And in Table 5, M_{max} increases as current velocity gets higher. On the contrary, T_{max} and T_{TDP} decrease.

4.2 Influence of top angle

In the laying process, top angle varies continuously to accommodate the variation of loads, which leads to a small bending moment at the top during the

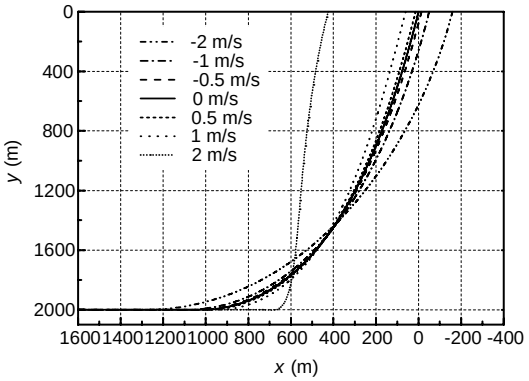

Fig. 12 Configuration of pipeline under different ocean currents

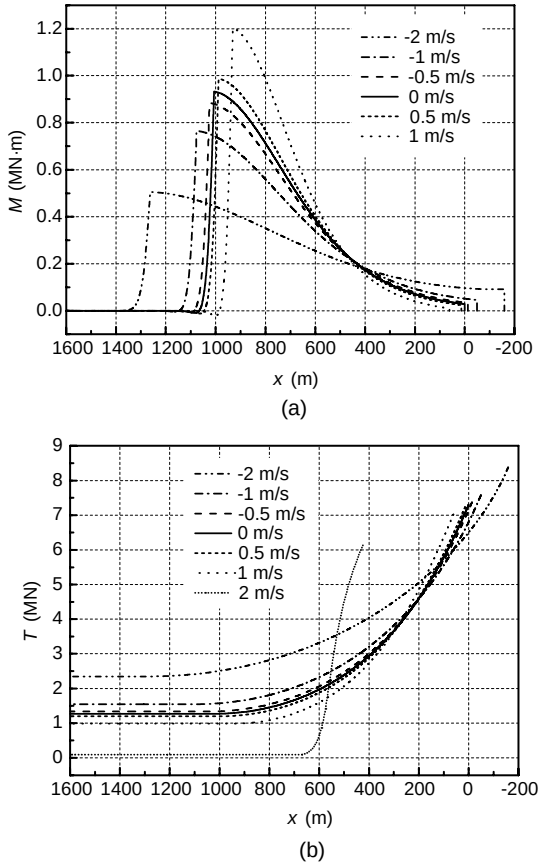

Fig. 13 Distribution of bending moment (a) and axial tension (b) under different ocean currents

Table 5 Critical loads for different current velocities

v_{max} (m/s)	M_{max} (MN·m)	T_{max} (MN)	T_{TDP} (MN)
−2	0.51	8.38	2.35
−1	0.77	7.58	1.55
−0.5	0.88	7.38	1.34
0	0.93	7.31	1.27
0.5	0.99	7.24	1.20
1	1.20	7.02	0.98
2	11.58	6.13	0.10

Table 6 Distance from TDP to the vessel and pipe embedment under different currents

v_{max} (m/s)	Distance (m)	e_{max} (m)	$e_{x\to\infty}$ (m)
−2	1263.3	0.51	0.51
−1	1076.6	0.53	0.51
−0.5	1024.5	0.54	0.51
0	1006.6	0.55	0.51
0.5	988.3	0.56	0.51
1	931.5	0.59	0.51
2	669.1	0.74	0.51

whole process. This is exactly one of the main advantages of the J-lay method. Fig. 14 shows the configuration of pipe for different top angles of 80°, 81°, 82°, 83°, 84°, 85°. The variation of loads is shown in Fig. 15. Other parameters are selected according to Table 1.

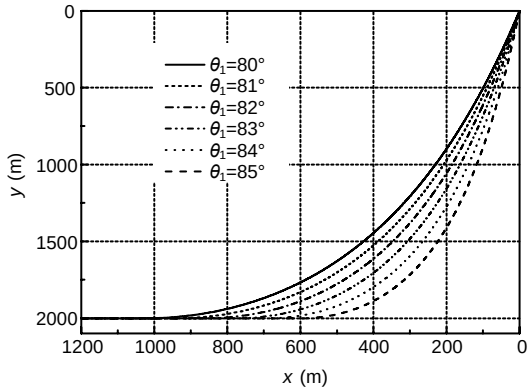

Fig. 14 Configuration of pipeline for different top angles

As the top angle increases, the distance between TDP and the laying vessel decreases, while the maximum pipe embedment grows rapidly, as shown in Table 7.

Table 8 indicates that the maximum bending moment M_{max} varies considerably for different top angles with a growing trend as the top angle gets larger. The decreases of T_{max} and T_{TDP} result from the shorter length of catenary part and smaller demand for horizontal force.

4.3 Influence of seabed stiffness

The stiffness of the seabed is important because it greatly influences the behavior of pipe at the neighborhood of TDP and the embedment of pipe laid on the seabed. Four types of soil with different shear strengths are selected: η=1.0, 1.5, 2.0, and 2.5 kPa/m. On the basis of Aubeny *et al*. (2005), the relationship between soil resistance and pipe embedment can be obtained. Then a linearly fitted relationship for each soil type can be achieved, as shown in Fig. 16 and Table 9.

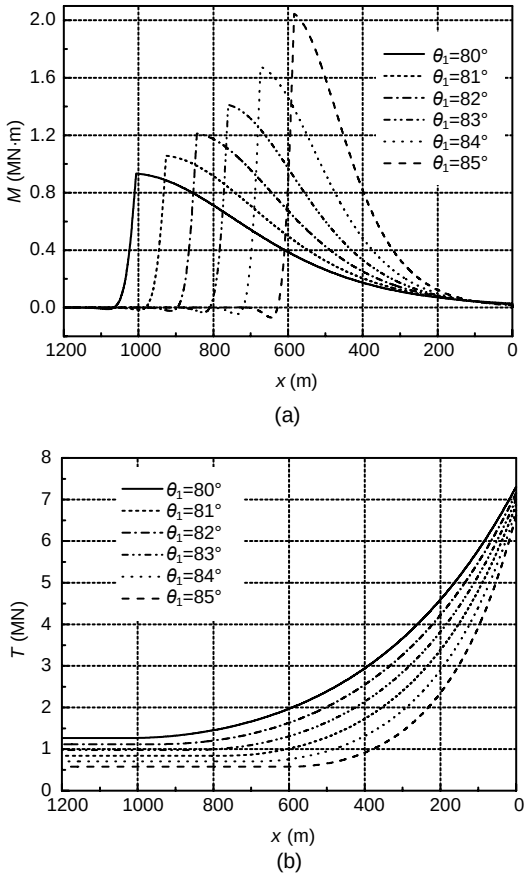

Fig. 15 Distribution of bending moment (a) and axial tension (b) for different top angles

Table 7 Distances from TDP to the vessel and pipe embedment for different top angles

θ_1 (°)	Distance (m)	e_{max} (m)	$e_{x\to\infty}$ (m)
80	1006.6	0.55	0.51
81	926.1	0.57	0.51
82	844.1	0.59	0.51
83	760.1	0.63	0.51
84	673.6	0.68	0.51
85	583.8	0.75	0.51

Table 8 Critical loads for different top angles

θ_1 (°)	M_{max} (MN·m)	T_{max} (MN)	T_{TDP} (MN)
80	0.93	7.31	1.27
81	1.06	7.16	1.12
82	1.21	7.01	0.98
83	1.41	6.88	0.84
84	1.68	6.74	0.71
85	2.05	6.61	0.58

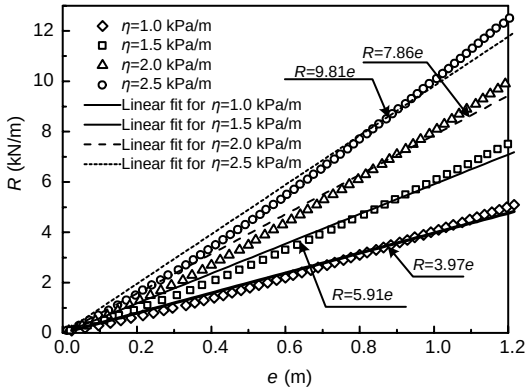

Fig. 16 Soil resistances and the fitting curves

Table 9 Seabed stiffness for different soil strengths

η (kPa/m)	1.0	1.5	2.0	2.5
Seabed stiffness (kN/m^2)	3.97	5.91	7.86	9.81

The influence on the configuration near TDP is shown in Fig. 17 where the embedment varies apparently for different seabed stiffness. As shown in Fig. 18 and Table 10, both e_{max} and $e_{x\to\infty}$ decrease with the increasing seabed stiffness, where $e_{x\to\infty}$ is controlled by the self-weight of pipe, and e_{max} is caused by its self-weight and the bending moment near TDP. In addition, Fig. 18 shows that e_{max} and $e_{x\to\infty}$ become closer when the seabed gets softer. It can be concluded that, when the seabed becomes softer, embedment near TDP becomes dominated by self-weight, and the bending moment has less influence on the pipe at the neighborhood of TDP. Table 11 shows that the internal loads vary little with the change of soil stiffness.

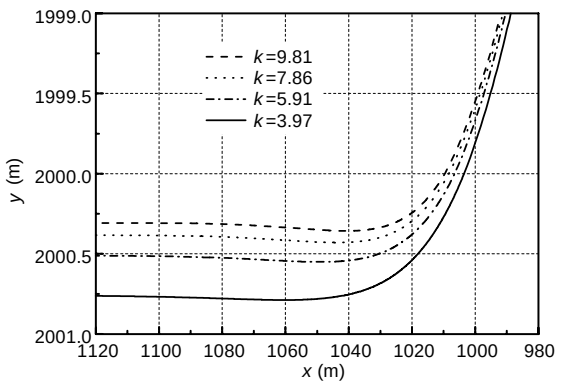

Fig. 17 Configuration of the neighborhood of TDP for different seabed stiffness

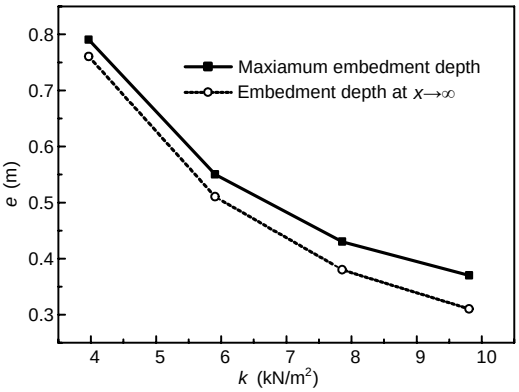

Fig. 18 Embedment for different seabed stiffness

Table 10 Embedment for different seabed stiffness

k (kN/m^2)	e_{max} (m)	$e_{x\to\infty}$ (m)
3.97	0.79	0.76
5.91	0.55	0.51
7.86	0.43	0.38
9.81	0.37	0.31

Table 11 Critical loads for different seabed stiffness

k (kN/m^2)	M_{max} (MN·m)	T_{max} (MN)	T_{TDP} (MN)
3.97	0.9323	7.3068	1.2703
5.91	0.9332	7.3063	1.2698
7.86	0.9336	7.3060	1.2695
9.81	0.9337	7.3058	1.2694

5 Conclusions

A simple numerical model for studying the static deployment of submarine pipes by the J-lay method is proposed. Such a numerical model has three main advantages. First, it is simple and easy to obtain the solution because there are only two variables in the whole calculation process. In addition, the influence of ocean currents and pipe embedment can be taken into account. Moreover, the solution requires just several seconds, so it is time-saving compared with the finite element method. In comparison with an analytical model, good agreement is found, which demonstrates that the solution of the numerical model is reliable.

The presented numerical model is applied to analyze the influence of different parameters, and some valuable conclusions can be drawn.

1. As water becomes deeper the maximum

bending moment becomes smaller, which is beneficial to the safety of pipelines. Yet, the increasing tension brings higher requirements on the capacity of the laying vessel. In addition, less embedment near TDP appears in deeper water, thus the pipe is more likely to move under thermal load, when transporting oil at high temperature.

2. When current velocity becomes larger, the bending moment along the pipe increases rapidly. This is absolutely different from pipe in calm water. For a current velocity of 2 m/s at the top, the maximum bending moment is far beyond control, which is very dangerous to the pipe. Thus, the influence of ocean currents must be taken into consideration. It is recommended to lay pipelines in good sea conditions, and the laying vessel needs to be powerful enough to resist rough sea conditions.

3. The steeper the top angle becomes, the smaller the required maximum axial force becomes, but the maximum bending moment becomes larger. So the top angle should be strictly controlled to make sure that both the axial tension and bending moment never exceed safe limits. The pipe embedment is also very important, and the maximum embedment of pipe increases for steeper top angles.

4. The seabed stiffness has a significant influence on the embedment of pipes, but very little influence on the internal loads. In addition, the bending moment at the neighborhood of TDP has less influence on the pipe if the seabed becomes softer. For muddy seabed, the catenary may give a good approximation for the overall pipeline.

The calculation results have proved the ability of the numerical model. However, some assumptions are made for the simplification in the above investigation, so further work needs to be carried out to ignore these assumptions, such as the consideration of 3D analysis and dynamic behaviors of pipe in currents.

References

Aubeny, C.P., Dunlap, W.A., 2003. Penetration of Cylindrical Objects in Soft Mud. Proc. IEEE Oceans, San Diego, CA, USA, p.2068-2073.

Aubeny, C.P., Shi, H., Murff, J.D., 2005. Collapse loads for a cylinder embedded in trench in cohesive soil. *International Journal of Geomechanics*, **5**(4):320-325. [doi:10.1061/(ASCE)1532-3641(2005)5:4(320)]

Aubeny, C.P., Biscontin, G., Zhang, J., 2006. Seafloor Interaction with Steel Catenary Risers. Final Project Report, Texas A&M University, USA.

Berteaux, H.O., 1976. Buoy Engineering. John Wiley and Sons, New York.

Brando, P., Sebastiani, G., 1971. Determination of Sealines Elastic Curves and Stresses to be Expected during Operation. Third Annual Offshore Technology Conference, Houston, Texas, OTC 1354.

Bridge, C., Laver, K., Clukey, E., Evans, T., 2004. Steel Catenary Riser Touchdown Point Vertical Interaction Models. Offshore Technology Conference, Houston, Texas, OTC 16628, p.1-8.

Burgess, J.J., 1994. The Deployment of an Undersea Cable System in Sheared Current. Proceedings of BOSS, **2**:327-334.

Casarella, M.J., Parsons, M., 1970. Cable systems under hydrodynamic loading. *Marine Technology Society Journal*, **4**(4):27-44.

Cheuk, C.Y., White, D.J., Dingle, H.R.C., 2008. Upper bound plasticity analysis of a partially-embedded pipe under combined vertical and horizontal loading. *Soils and Foundations*, **48**(1):133-140.

Dixon, D.A., Rultledge, D.R., 1968. Stiffened catenary calculation in pipeline laying problem. *Journal of Engineering for Industry*, **90**B(1):153-160.

Guarracino, F., Mallardo, V., 1999. A refined analytical analysis of submerged pipelines in seabed laying. *Applied Ocean Research*, **21**(6):281-293. [doi:10.1016/S0141-1187(99)00020-6]

Langner, C.G., 1984. Relationships for Deepwater Suspended Pipe Spans. Proc. Offshore Mechanics and Arctic Engineering Symposium, New Orleans, Louisiana, p.552-558.

Lenci, S., Callegari, M., 2005. Simple analytical models for the J-lay problem. *Acta Mechanica*, **178**(1-2):23-39. [doi:10.1007/s00707-005-0239-x]

Li, Z.G., Wang, C., He, N., Zhao, D.Y., 2008. An overview of deepwater pipeline laying technology. *China Ocean Engineering*, **22**(3):521-532.

Liang, Z.T., 2008. Analysis on Mechanical Performance for Deep-water Pipe-laying. MS Thesis, Zhejiang University, China (in Chinese).

Merifield, R.S., White, D.J., Randolph, M.F., 2008. The ultimate undrained resistance of partially embedded pipelines. *Géotechnique*, **58**(6):461-470. [doi:10.1680/geot.2007.00097]

Merifield, R.S., White, D.J., Randolph, M.F., 2009. Effect of surface heave on response of partially embedded pipelines on clay. *Journal of Geotechnical and Geoenvironmental Engineering*, **135**(6):819-829. [doi:10.1061/(ASCE)GT.1943-5606.0000070]

Morison, J.R., O'Brien, M.P., Johnson, J.W., Schaaf, S.A., 1950. The Force Exerted by Surface Waves on Piles. Petroleum Transactions, AIME, **189**:149-154.

Murff, J.D., Wanger, D.A., Randolph, M.F., 1989. Pipe penetration in cohesive soil. *Géotechnique*, **39**(2):213-229. [doi:10.1680/geot.1989.39.2.213]

Palmer, A.C., Hutchinson, G., Ells, W.J., 1974. Configuration of submarine pipelines during laying operations. *Journal*

of Engineering for Industry, **96**(4):1112-1118.

Perinet, D., Frazer, I., 2007. J-lay and Steep S-lay: Complementary Tools for Ultra Deep Water. Houston, Texas, OTC 18669.

Plunkett, R., 1967. Static bending stresses in catenaries and drill strings. *Journal of Engineering for Industry*, **39**B(1):31-36.

Powers, J.T., Finn, L.D., 1969. Stress Analysis of Offshore Pipelines during Installation. First Annual Offshore Technology Conference, Houston, Texas, OTC 1071.

Pulici, M., Trifon, M., Dumitrescu, A., 2003. Deep Water Sealines Installation by Using J-lay Method—The Blue Stream Project. Proceedings of the Thirteenth International Offshore and Polar Engineering Conference, Honolulu, Haiwaii, p.38-43.

Vaz, M.A., Paten, M.H., 2000. Three-dimensional behavior of elastic marine cables in sheared currents. *Applied Ocean Research*, **22**(1):45-53. [doi:10.1016/S0141-1187(99)00023-1]

Wasow, W., 1956. Singular perturbations of boundary value problems for nonlinear differential equations of second order. *Communications on Pure and Applied Mathematics*, **9**(1):93-113. [doi:10.1002/cpa.3160090107]

Wilson, B.W., 1960. Characteristics of Anchor Cables in Uniform Ocean Currents. Technical Report No. 204-1, Texas A&M University, USA.

Zhou, J., 2008. Investigation on Configuration and Construction Technics of S-lay for Deepwater Submarine Pipelines. MS Thesis, Zhejiang University, China (in Chinese).